Research Article

Alejandro Martinez Gordon*, María Isabel Prieto Barrio, and Alfonso Cobo Escamilla

Graphene nanofibers: A modern approach towards tailored gypsum composites

https://doi.org/10.1515/ntrev-2022-0559 received October 31, 2022; accepted May 19, 2023

Abstract: Energy poverty is a global challenge that demands sustainable and affordable solutions. This study investigates the use of commercial graphene nanofibers (GNFs) as a reinforcing agent in gypsum composites for energy-efficient building retrofitting. The GNFs were manually dispersed in the gypsum matrix, and the composites were fabricated by casting and curing. The thermomechanical properties were systematically studied using various characterization techniques, including scanning electron microscopy, X-ray diffraction, and thermal analysis. The results show that the addition of 1% GNFs reduces the thermal conductivity of the composites by more than 40% and improves their flexural and compressive strength by up to 23 and 42%, respectively, compared to neat gypsum. The enhancements are attributed to the effective phonon scattering of the GNFs and their ability to act as crystal seeding sites, resulting in a denser and more homogeneous structure. The dynamic thermal analysis further demonstrates that the GNF-reinforced composites could reduce heating and cooling requirements by 14 and 11%, respectively, indicating their potential for energy-efficient building retrofitting. However, the cost effectiveness and safety issues of the GNF-reinforced composites should be carefully considered before their large-scale implementation. Achieving uniform dispersion of nanoparticles in high concentrations is also a significant challenge that will be addressed in future studies.

Keywords: gypsum, graphene nanofibers, energy poverty, phonon-scattering, crystal seeding

María Isabel Prieto Barrio, Alfonso Cobo Escamilla: Universidad Politécnica de Madrid, Escuela Técnica Superior de Edificación, 28050 Madrid, Spain

1 Introduction

The construction industry is a major contributor to greenhouse gas emissions and energy consumption, which is especially concerning in developed countries, where it accounts for 40% of energy consumption and emissions. This contributes to energy poverty and environmental degradation. As a result, sustainable practices are becoming increasingly important in the industry. Gypsum-based materials (CaSO₄·2H₂O) have emerged as a promising solution due to their abundant availability, eco-friendly properties, and affordability. However, the durability and resistance of gypsum-based materials are critical features that affect their lifespan and performance [1–8].

In recent years, many studies have aimed to develop gypsum-based composites with lower environmental impacts and improved thermal and acoustic properties. However, these developments have come at the cost of reduced mechanical properties, as observed by researchers, and documented in Table 1. Various additives, such as expanded polystyrene (EPS) [9], polypropylene fibers (PP) [10], polyamide fibers (PA) [11], textile fibers [12], cellulose fibers [13], chicken feathers [14], copper slags [15], graphite [16], and even rubber particles [17], have been explored to enhance the physical and mechanical attributes of these composites. Nonetheless, it has been observed that these additives can adversely affect the bonding between the gypsum matrix and the additives, particularly at higher concentrations. As a result, the most promising outcomes have been achieved at low additive concentrations (less than 10%) and by employing a w/g ratio of 0.65–0.75.

While the use of wastes and other additives has shown promise in improving the physical and thermal properties of gypsum-based composites, there is still room for improvement. Carbon nanomaterials (NMT) such as carbon nanotubes (CNTs) and graphene have garnered attention in the building industry for their ability to provide new applications and improve the overall quality and characteristics of common materials [18–22].

Given their small size, these materials exhibit increased reactivity, greater surface area, and distinct characteristics

^{*} Corresponding author: Alejandro Martinez Gordon, Universidad Politécnica de Madrid, Escuela Técnica Superior de Edificación, 28050 Madrid, Spain, e-mail: a.mgordon@alumnos.upm.es

compared to materials at a larger scale. Previous studies have observed that CNTs can increase crystallization centers in a gypsum matrix, contributing to a denser matrix and improved electronics properties, which could be beneficial in terms of electromagnetic shielding or sensing. However, exceeding the optimal value resulted in a decrease in mechanical properties due to the formation of a structure with higher porosity [23–27].

As such, the implementation of nanomaterials (NMTs) in construction presents several challenges including issues with availability, consistency, quality, market trends, dispersion issues, and cost. The use of NMTs in large quantities also raises concerns about potential health and environmental risks, limiting their widespread implementation in the industry. To overcome these challenges, researchers suggest using low concentrations, ranging from 0.001 to 1%. This approach helps to prevent negative impacts on the properties, cost, and recyclability of the composite [1,18–22].

To date, there is limited research on the use of graphene nanofibers (GNFs) in gypsum composites, and their impact on the properties of these materials. GNFs are a promising candidate due to their high aspect ratio, large surface area, and excellent mechanical, thermal, and electronic properties. GNFs have already been shown to improve the strength and durability of isotactic polypropylene (iPP), offering potential applications in various fields such as electronics, energy, and biomedicine [18,27,28].

The present study developed an eco-friendly and safe gypsum composite that incorporated GNFs to improve their mechanical and thermal properties while examining the potential risks and costs associated with their use. The incorporation of GNFs in gypsum composites could lead to the development of tailored building materials and retrofits that meet market requirements, such as controlled porosity,

high or low thermal conductivity, electromagnetic shielding, carbon capture, and building monitoring. The physical and mechanical properties of the composites were evaluated, including their strength, hardness, thermal conductivity, water absorption, porosity, and their thermal values were used to assess their performance in a typical southern Spanish dwelling. Furthermore, this study also examined the dispersion issues and potential risks associated with low concentrations of GNFs in order to ensure their proper implementation in the construction industry. These results could provide a better understanding of how GNFs affect the properties of gypsum composites and contribute to existing knowledge in this area.

2 Materials and methods

2.1 Materials

The present work designed a gypsum composite using GNFs as a reinforcing agent. Commercial building gypsum type B1-YG/L from PLACO-Saint Gobain was used as a matrix, while the GNFs-LS class was supplied by the company Graphenano, located in Murcia, Spain. Technical specifications of both raw materials are shown in Table 2.

2.2 Experimental procedure

Composites were elaborated by manually mixing up to 1% of GNFs with dry-building gypsum until a well-dispersed distribution was achieved. GNFs were handled at all times

Tab	le '	1:	Summary	of	properties	of	gypsum-	based	composites	obtai	ned	from t	he	iterature
-----	------	----	---------	----	------------	----	---------	-------	------------	-------	-----	--------	----	-----------

Author	Year	Additive	%	w/g	Density (kg/m³)	Flexural strength (Mpa)	Compressive strength (Mpa)	λ (W/mK)
Bouzit et al. [9]	2021	EPS	10	0.80	*	3.4	1	0.191
Eve <i>et al.</i> [11]	2002	PA fiber	5	0.68	*	2	6	*
Vasconcelos et al. [12]	2015	Cork/textiles	7/3	0.88	714	*	2.13	*
Serna <i>et al.</i> [17]	2012	Rubber particles	5	0.70	*	3.26	5.54	*
Barbero-Barrera et al. [16]	2017	Graphite	15	0.74	1,190	*	4.8	0.600
Flores Medina and Barbero- Barrera [10]	2017	PP fibers	0.6	0.60	940	0.50	0.98	0.167
Hagiri and Honda [15]	2021	Copper slag	20	0.67	1,010	2.57	*	*
Ouakarrouch <i>et al.</i> [14]	2020	Chicken feathers	5	0.60	1048.9	*	*	0.309
Senff et al. [13]	2018	Cellulose/n-TiO ₂	2/1	0.37	*	0.48	*	0.770
Gordina <i>et al.</i> [18]	2013	CNT	0.001	0.60	*	4	15	*

^{*}Not provided.

Table 2: Technical specifications of building gypsum type B1-YG/L and GNFs

Material	Density (g/cm³)	Melting point (°C)	Particle size	Electrical resistivity (Ωm)	λ (W/mK)
Building gypsum B1 YG/L	2.3	100–150	≤1 mm	3.4 × 10 ⁴	0.34
GNFs-LS	0.2-0.3	3650 -3,700	≥20 nm	4.6×10^{-6}	1,400-1,600

with the proper individual protection equipment, including safety glasses, facemasks, and gloves. All samples presented a w/g of 0.75, determined in accordance with European regulation EN 13279 [29,30]. Water was added to the dry mixture, and the resulting slurry was then casted in $40 \times 40 \times$ 160 mm³ molds, as seen in Figure 1. After 1 h, the samples were removed from the molds and were kept at room conditions for 7 days before testing. The composition of each sample is listed in Table 3.

2.3 Physical and mechanical properties

The bulk density and the void content (V_c) were determined through the Archimedes method. The immersion absorption coefficient (W_{Abs}) was also measured at 24 h, following the indications of the EN 13279-2:2014 standard [50]. $V_{\rm c}$ and $W_{\rm Abs}$ were determined using equations (1) and (2), respectively,

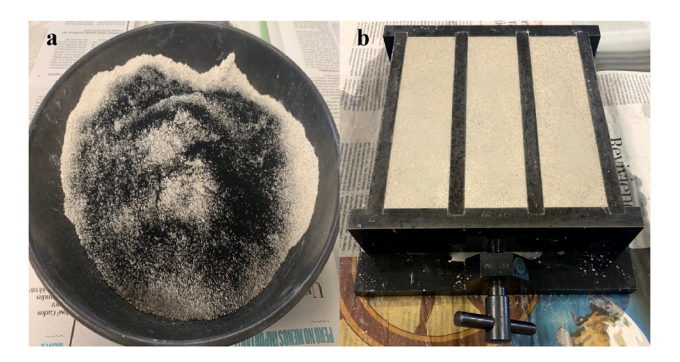


Figure 1: Dry mixture of gypsum and GNFs (a) and mold containing casted slurry (b).

Table 3: Designation and detailed composition of each mixture

Sample	GNFs (%)	Gypsum (g)	Water (g)	GNFs (g)	w/g
Ref	0	800	600	0	0.75
LS-0.25	0.25	800	600	2	0.75
LS-0.50	0.50	800	600	4	0.75
LS-0.75	0.75	800	600	6	0.75
LS-1.00	1.00	800	600	8	0.75

$$V_{c(\%)} = \left[\frac{w_{\rm S} - w_{\rm d}}{w_{\rm d} - w_{\rm sub}} \right] \times 100, \tag{1}$$

$$W_{\text{Abs(\%)}} = \left[\frac{w_{\text{s}} - w_{\text{d}}}{w_{\text{d}}} \right] \times 100, \tag{2}$$

where w_s represents the saturated weight after 24 h of immersion, w_{sub} is the submerged weight, and w_{d} is the dry weight of the samples after retrieving them from the stove. Crystal size, morphology, and structure of the composites were also studied by means of scanning electron microscopy (SEM). Energy dispersive spectrometry (EDS) was used to examine the local elemental composition while observing the samples. Crystalline phases present in the composites were determined by means of X-ray diffraction (XRD) using a Bruker D8 ADVANCE diffractometer.

The values of hardness index at the Shore C scale, flexural and compressive strength were obtained in accordance with the EN 13279-2:2014 standard [30]. Values for superficial hardness were obtained after taking a total of 18 measurements, 6 for each smooth side of the sample. Flexural and compressive strength were measured using a universal testing machine IBERTEST MIB60-AM with a preload of 0.5 kN and a loading rate of 10 mm/min, as shown in Figure 2. For each designation, three identical samples were tested, and the average value was reported.

Thermal conductivity testing was performed at the physics laboratory located in the school of building engineering of the Technical University of Madrid. Thermal properties were measured using a 400 × 400 × 400 mm³ insulating cube used in other studies [10,31,32]. Samples



Figure 2: Flexural test (a) and insulating cube employed to measure thermal properties (b).

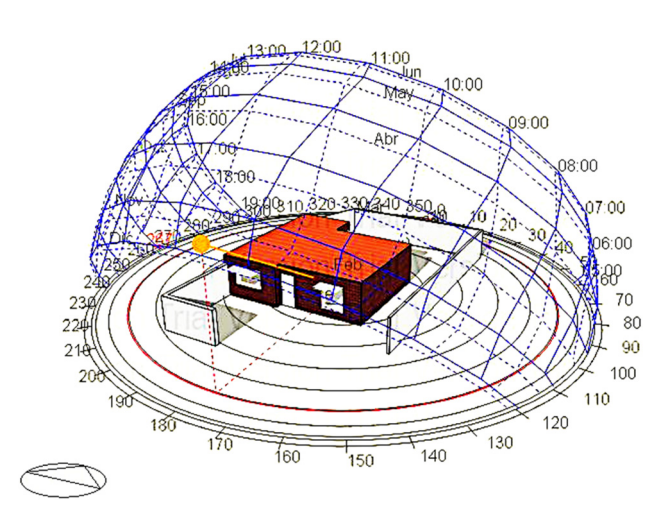


Figure 3: Simulated building model, solar trajectory, and shades.

were fixed in the $21 \times 21 \text{ cm}^2$ openings located on each wall; afterwards, they were sealed from external conditions by adding a 3 cm EPS board. The stationary state was reached 5 h after placing the samples in the cube. Thermocouples recorded the temperature in a 30 min span, and the thermal conductivity was determined using Fourier's law.

2.4 Dynamic thermal simulation

This section presents the simulation of environmental and energy-saving characteristics when gypsum plasterboards with and without GNFs are implemented as retrofit components in a poorly insulated dwelling. The simulations took place using the Energy plus module within the Design Builder software. Yearly consumption values (kWh), utility use per total area (kWh/ m^2), and CO₂ emissions (kg) were obtained for all envelope arrangements.

The building studied is a typical Spanish dwelling in the city of Almería, situated in southern Spain, 21 m above sea level in the Mediterranean basin. Almería is known for its year-round dry environment with very warm winters

Table 4: Parameter settings for the studied dwelling

Location	Almería, Spain
Total area (m²)	72
Occupancy (Hab/m²)	0.0277
Window type	Preferred height, 30% glazed
Shading	Blinds w/high reflectivity
Local shading	1 m Overhang
Humidity control	Dehumidification
Lighting type	Suspended
Power density (W/m ²)	5.0

Table 5: Original building components and thermal properties of the simulated building model

Component	Material	Thickness (m)	λ (W/mK)
External wall	Outer bricks	0.100	0.840
	Hollow concrete bricks	0.200	0.480
	Gypsum plasterboard	0.030	0.341
Roof	Roofing tiles	0.016	0.840
	Asphalt	0.010	0.300
	Concrete roofing slab	0.145	0.160
	Gypsum plasterboard	0.025	0.341
Partitions	Gypsum plasterboard	0.025	0.341
	Hollow concrete bricks	0.080	0.480
	Gypsum plasterboard	0.025	0.341
Inner floor	Timber flooring	0.015	0.140
	Gypsum plasterboard	0.025	0.341
	Concrete slab	0.250	0.380

and low precipitation. A model of the building consisting of one floor and a total area of $72\,\mathrm{m}^2$ is shown in Figure 3. Parameter settings and building components are listed in Tables 4–7. For this home, a yearly heating and cooling schedule was selected. The system was activated when the indoor temperature fell below 18°C during winter and exceeded 25°C during the summer.

3 Results and discussion

3.1 Physical and mechanical properties

The workability and initial setting times of the samples were not affected by adding GNFs and remained above

Table 6: Building components including 1% gypsum-GNFs composites as insulating surfaces

Component	Material	Thickness (m)	λ (W/mK)
External wall	Outer bricks	0.100	0.840
	Hollow concrete bricks	0.200	0.480
	Gypsum-GNF 1%	0.030	0.199
Roof	Roofing tiles	0.016	0.840
	Asphalt	0.010	0.300
	Concrete roofing slab	0.145	0.160
	Gypsum-GNF 1%	0.025	0.199
Partitions	Gypsum-GNF 1%	0.025	0.199
	Hollow concrete bricks	0.080	0.480
	Gypsum-GNF 1%	0.025	0.199
Inner Floor	Timber flooring	0.015	0.140
	Gypsum-GNF 1%	0.025	0.199
	Concrete slab	0.250	0.380

Table 7: Building components including the benefits of both 0.50 and 1% gypsum-GNFs composites

Component	Material	Thickness (m)	λ (W/mK)
External wall	Outer bricks	0.100	0.840
	Hollow concrete bricks	0.200	0.480
	Gypsum-GNFs 1%	0.030	0.199
Roof	Roofing tiles	0.016	0.840
	Asphalt	0.010	0.300
	Concrete roofing slab	0.145	0.160
	Gypsum-GNFs 1%	0.025	0.199
Partitions	Gypsum GNFs 1%	0.025	0.199
	Hollow concrete bricks	0.080	0.480
	Gypsum GNFs 1%	0.025	0.199
Inner floor	Timber flooring	0.015	0.140
	Gypsum-GNFs 0.5%	0.025	0.574
	Concrete slab	0.250	0.380

50 min. There were no issues with sedimentation or dispersion during the entire process, and no signs of detachment or loss of material were detected when handling the samples. However, the color of the composite turned gray as the concentration of GNFs in the mixture increased. Nevertheless, since GNF content was low, it is not expected to have a negative impact on the recyclability of common gypsum since GNFs are unaffected by thermal treatments. The hemihydrate powder containing GNFs can then be reconstituted into Gypsum-GNF composites by adding water to the mixture and casting the slurry into molds.

In Table 8, the results for bulk density, void content, and water absorption are given. It can be seen that the bulk density increases with GNF concentration up to 6%, obtaining values within the range of common gypsum-based products, usually oscillating between 700 and 1,100 kg/m³ [33].

The void content decreased by approximately 2% in samples that contained GNFs. The highest void content was observed in the reference sample, whereas the lowest belonged to the composite containing 0.50% GNFs. A slight reduction in void content was expected since GNFs can fill the microstructure to some extent. These voids are the result of entrapped gas molecules that continuously forms

bubbles and will only be ejected from the mixture by periodic and gentle agitation of the molds or if the size and growth kinetics of the bubbles allows them to reach the liquid-air interface before setting takes place [34].

Water absorption by immersion was also reduced by introducing carbon NMT in the mixture, reaching values, on average, 4% lower than those obtained by the reference sample. This reduction is a direct consequence of the concurrent filling and densifying effects of GNFs when introduced to the calcium sulfate matrix. This type of behavior has also been observed with different additives and other binders, as the introduction of well-dispersed additives can refine the bulk density, durability, and pore structure in traditional materials providing additional features in the process. However, higher concentrations are known to cause agglomerations, poor bonding, and workability due to their uneven distribution within the mixture [7,10,16,18,35-37].

Building materials play a vital role in this modern era; although usually considered for construction works, most applications will require these materials to function properly. In addition, their capacity, quality, and implementation are generally dictated by their own properties. Surface hardness, flexural, and compressive strength are among the most important attributes in building materials, and the values for these features are also expressed in Table 8.

Neat gypsum reached values for flexural and compressive strength of 2.30 and 4.06 MPa, respectively. While all composite samples presented a steady increase in GNF content in both flexural and compressive strength, as expressed in Figures 4 and 5. Samples containing 1% of GNF's achieved the highest values for flexural and compressive strength with increments of 23 and 42%, in comparison to common gypsum. As a result, these composites are lighter and required less amounts of additive to achieve greater values for compressive strength when compared to gypsum samples containing isostatic graphite [16].

Strength in gypsum products stems from several reasons, such as binder and additive quality, w/g ratio, curing conditions, and porosity. That said, it is worth noting that all studied properties were in total compliance with the

Table 8: Physical and thermomechanical properties of different gypsum samples

Sample	Bulk density (kg/m³)	V _c (%)	W _{Abs} (%)	Shore C hardness index	Flexural strength (MPa)	Compressive strength (MPa)	λ (W/mK)
Ref	1,031	40.6	39.4	65 ± 4	2.30 ± 0.07	4.06 ± 0.01	0.341
LS-0.25	1,063	39.4	37.0	66 ± 5	2.37 ± 0.09	4.56 ± 0.05	0.372
LS-0.50	1,095	38.5	35.1	70 ± 3	2.61 ± 0.03	5.20 ± 0.01	0.574
LS-0.75	1,094	38.7	35.4	73 ± 5	2.71 ± 0.02	5.37 ± 0.01	0.327
LS-1.00	1,092	39.0	35.7	75 ± 5	2.82 ± 0.03	5.77 ± 0.03	0.199

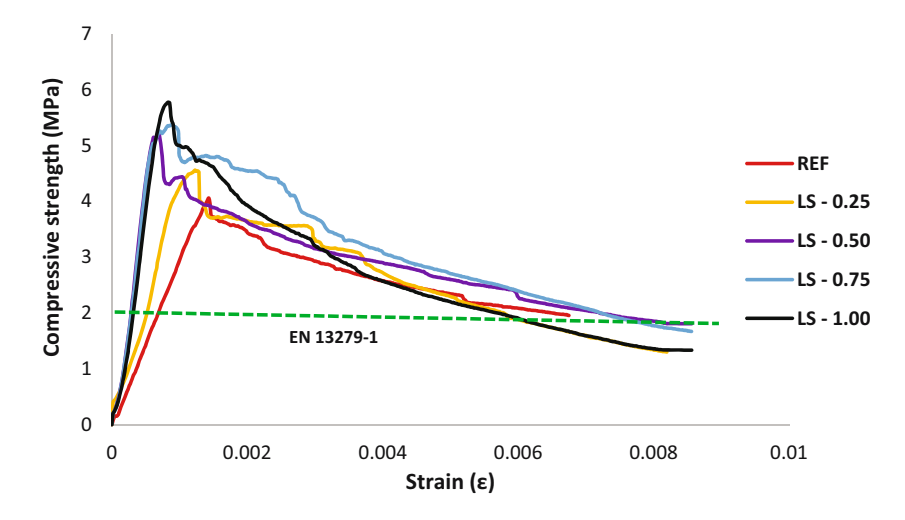


Figure 4: Stress-strain curves of all studied samples.

requirements, as well as the criteria, established by Spanish standard EN 13279-1 and Lushnikova *et al.* [8,29]. However, most properties of gypsum products and building materials will mainly be determined by the structure of their matrix [4,9,38].

3.2 Morphology and composition analysis (SEM and XRD)

Microstructural analysis revealed that samples without GNFs presented needle-like crystals spread along the matrix with an average size of $21.4\,\mu m$, as seen in Figure 6. In this case, the structure displayed a higher amount of porosity that resulted in lower durability and mechanical properties, in comparison

to other samples. When GNFs are implemented in the mixture, an ordered and uniform structure emerges with longer crystals, decreased porosity, and improved mechanical properties.

These nanodispersed additives, as in other works, acted as crystallization centers introducing excess energy into the system, hence, improving crystal seeding and growth rate. More contact and interaction within the crystals translates into a higher overall strength of the composite, resulting in a denser, durable, and stronger matrix. Therefore, GNFs prove to be a viable option to modify and regulate, to some extent, the properties of traditional materials such as gypsum, paving the road for new tailored composites specifically designed to address certain market needs [18,19,39,40].

While studying these NMT, it was revealed that they present themselves as clusters along the gypsum matrix,

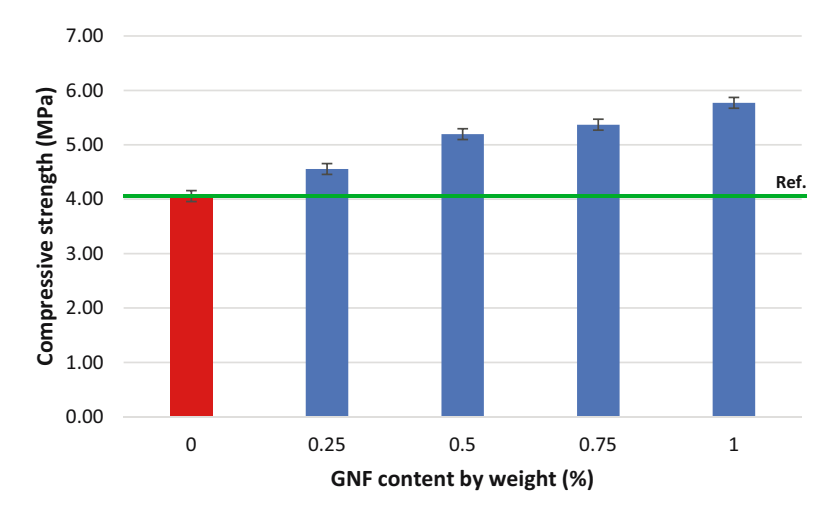


Figure 5: Compressive strength in the function of GNF content in the mixture.

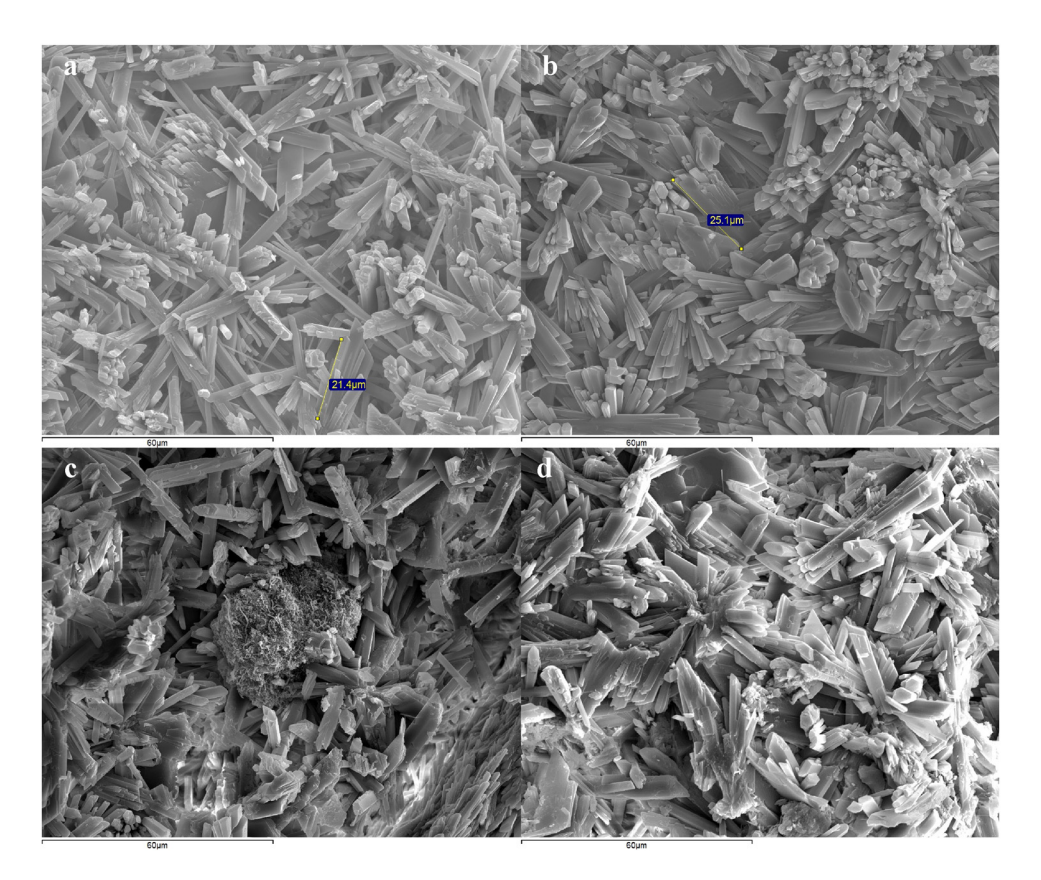
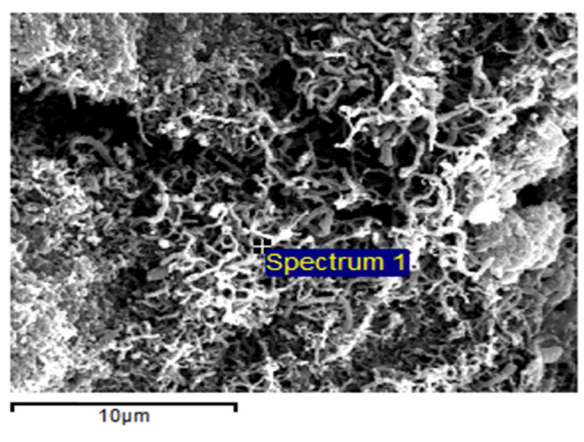


Figure 6: Microstructural analysis (1,000×) of the reference sample (a) and samples containing 0.25% (b), 0.50% (c), and 1% (d) of GNFs.



DE GRUYTER

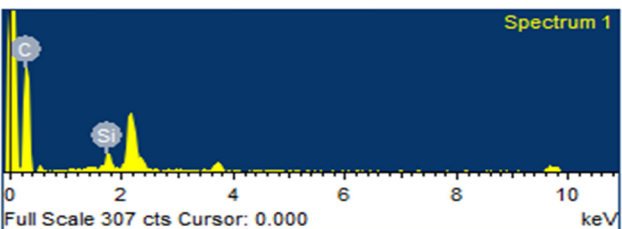
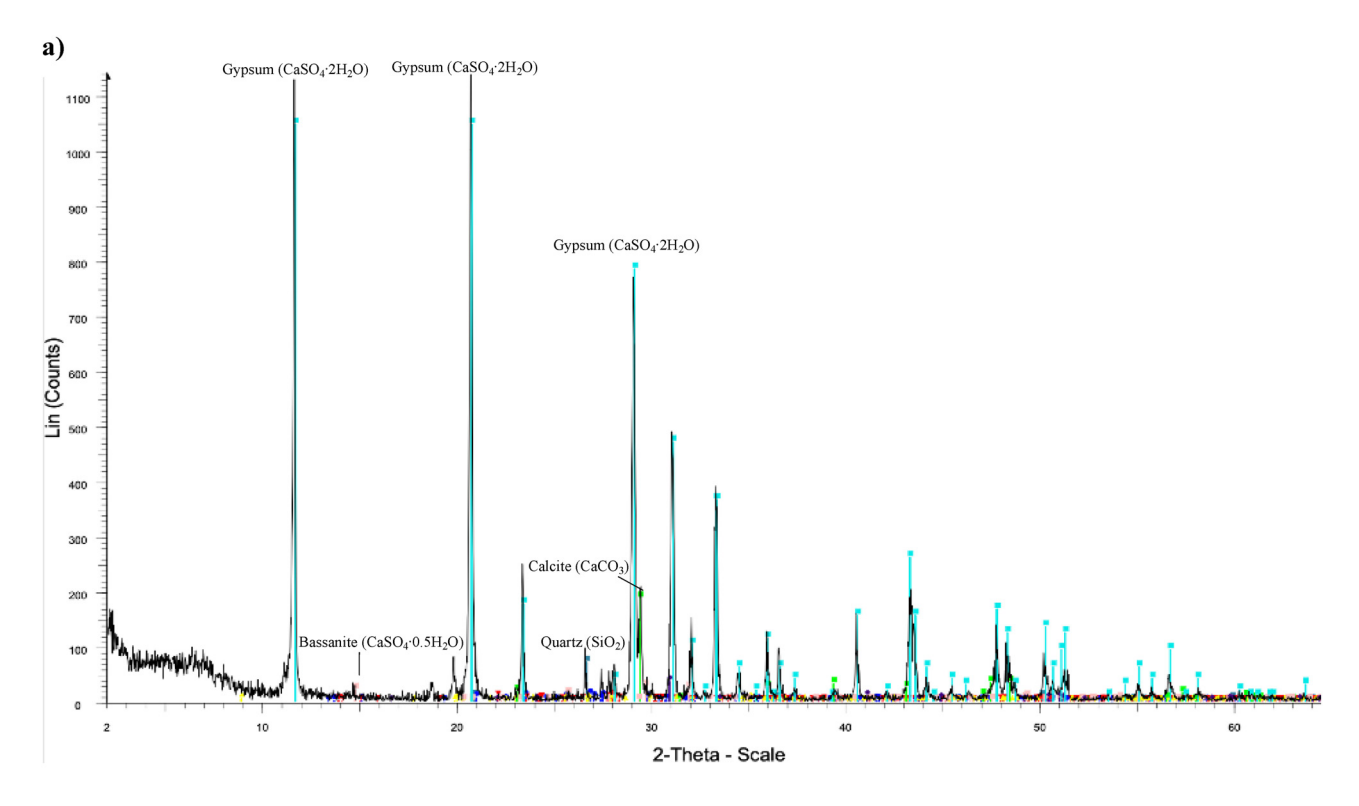


Figure 7: Microstructure and EDS analysis of GNFs (5,000×).

with filaments of several nanometers in length, as shown in Figure 7. Furthermore, small amounts of Si (<4%) were detected to be present within GNFs, which might indicate that silicon carbide (SiC) wafers were employed as a production method to produce this graphene additive. Since graphitic layers are known to be grown either on the silicon or carbon faces of a SiC wafer by sublimating Si atoms, thus leaving a graphitized surface. The quality of such graphene can be very high, with crystallites approaching hundreds of micrometers in size. Unfortunately, due to high temperatures, high substrate cost, and small-diameter wafers, the use of graphene on SiC will probably be limited to lowrequirement applications [26,41,42].

XRD analysis was performed exposing changes in the crystalline phases present in the test samples. Patterns of samples with and without additives are shown in Figure 8. The main reflections correspond to the peaks of gypsum (CaSO₄·2H₂O) followed by calcite (CaCO₃), quartz (SiO₂), bassanite (CaSO₄·½H₂O), dolomite (CaMg (CO₃)₂), along with lower quantities of alkali-feldspars and phyllosilicates, as seen in Table 9.



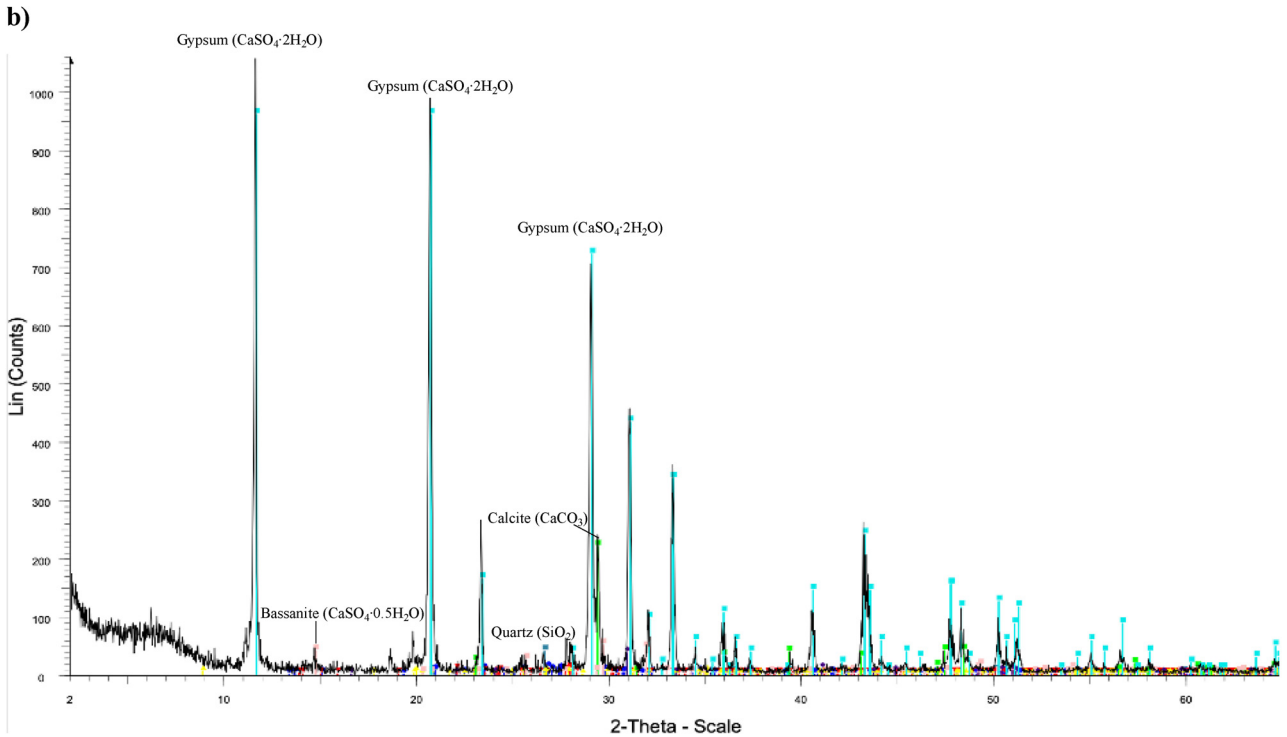


Figure 8: XRD patterns for the reference sample (a) and the composite containing 0.50% GNFs (b).

No carbon peaks were detected due to our additive being highly amorphous, hence, poorly detectable by our equipment. When compared, it was revealed that, when GNFs are introduced, the intensity of reflections for gypsum slightly

drops while those of bassanite tend to increase in all samples $(2\theta \approx 15)$, indicating a frail drop in hydration conditions.

Nanoparticles are generally characterized as being highly reactive and hydrophobic; thus, an increase in the

Table 9: Crystalline	phases	present in all	samples b	y means of XRD
----------------------	--------	----------------	-----------	----------------

Sample	SiO ₂	KAISi ₃ O ₈	NaAlSi₃O ₈	KAl ₂ (AlSi ₃ O ₁₀)(OH) ₂	CaCO ₃	CaMg(CO ₃) ₂	CaSO ₄ ·½H ₂ O	CaSO ₄ ·2H ₂ O
Ref	3.0	2.1	2.1	2.2	8.0	2.0	2.1	78.5
LS-025	2.1	2.2	2.2	2.2	8.9	2.0	2.1	78.3
LS-050	1.7	2.0	2.1	2.0	9.9	2.0	4.1	76.2
LS-1.00	1.8	2.0	2.1	2.0	11.1	2.2	3.1	75.7

intensity peaks for bassanite can be explained by a drop in hydration conditions. On this matter, Wigley [38] mentions that a decrease in the solubility of gypsum, at any temperature, is to be expected when applying other minerals or additives in the mixture. Therefore, introducing higher concentrations of this additive (>1%) could seriously affect the overall performance of the composites if no changes are implemented in the mixture to ensure proper particle distribution and hydration [18,19,21,22].

3.3 Thermal properties

In Figure 9, the values for thermal conductivity (λ) at different concentrations of GNFs are presented. The reference sample achieved a value of 0.341 W/mK, while those containing 0.50% of GNFs reached a value of 0.574 W/mK; thus, an increase of almost 70% was achieved at very low percentages. Hence, when this type of additive is employed in very small amounts, λ will tend to increase progressively.

However, as GNF content continues to increase within the mixture, a sudden drop in thermal conductivity was reported. Incorporating 1% of these NMT resulted in a remarkable reduction in λ by more than 40%, reaching a value of 0.199 W/mK. In contrast, these values for thermal conductivity remained within the range of those obtained by implementing 10% of EPS or silica granules without compromising mechanical properties [4,33,43].

This reduction in λ may be due to the effects of intensified phonon scattering, as shown in Figure 10. Since thermal energy in insulating solids is mainly transported by these quasiparticles, whose interactions with impurities, interfaces, or other phonons can produce different scattering events of this incident energy. Thus, heat transport along these composites can be regulated by employing nanoparticles such as GNFs. These composites could be implemented in new proposals or retrofits as false ceilings, internal walls, or even heating tiles depending on the GNF content [44–46].

By refining the thermal features of common materials, we could further address user comfort, as well as reduce heating and cooling requirements. This could be a first step toward mitigating the current difficulties established by EP, since energy prices, inflation, occupancy, and residential demands have risen while incomes and employment rates have lowered due to the persisting effects of COVID-19 and nearby conflicts [2,47,48]

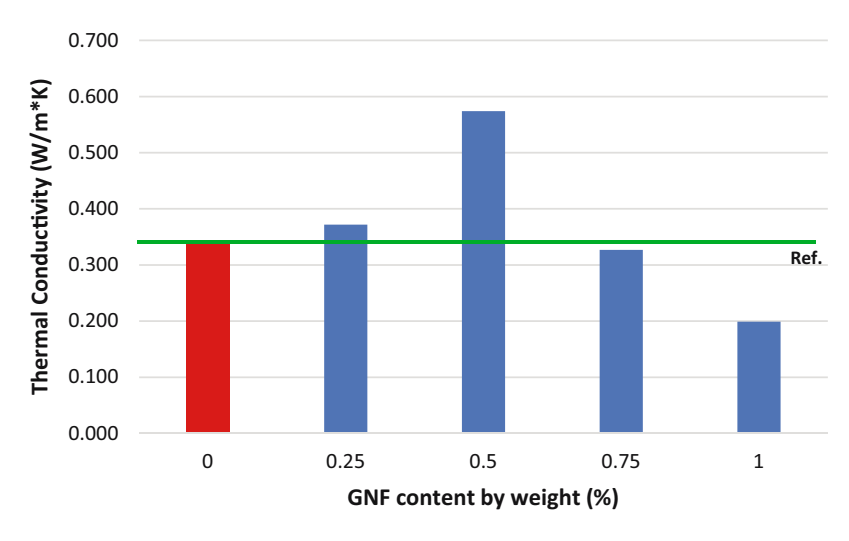


Figure 9: Thermal conductivity in the function of GNF content.

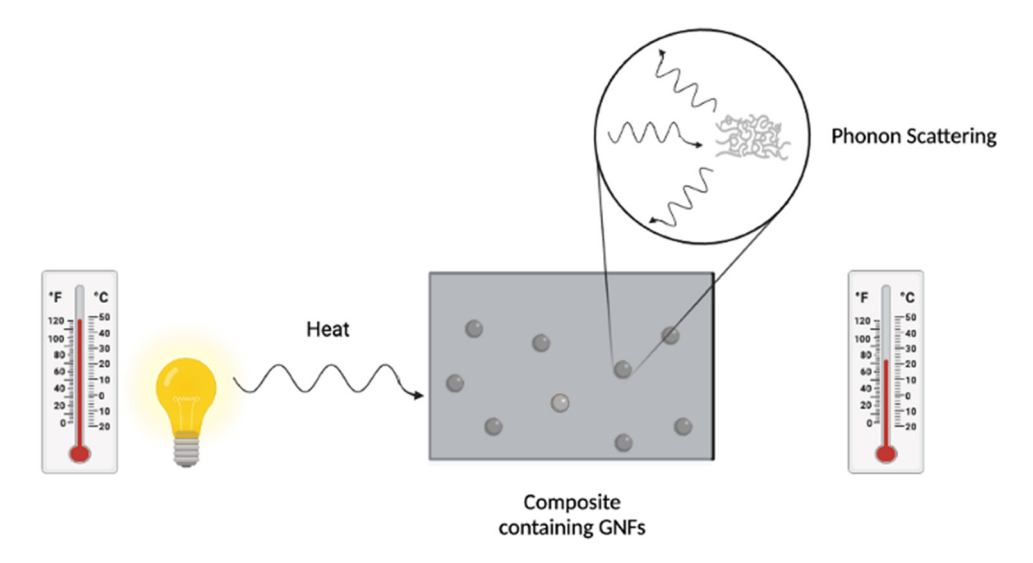


Figure 10: Phonon scattering events in gypsum composites containing GNFs. Own image-Biorender.

Table 10: Dynamic thermal simulation results of a building in Almeria implementing different arrangements

Arrangement	Heating requirements (kWh/year)	Cooling requirements (kWh/year)	CO ₂ emissions (kg/year)	Total energy per building area (kWh/m²)
Reference	2060.5	1291.4	1804.3	62.2
Gypsum-GNFs 1%	1827.8	1108.2	1608.8	56.6
Gypsum GNFs 0.50 and 1%	1925.3	1223.1	1717.4	60.2

3.4 Dynamic thermal analysis

Andalusia is one of Spain's most populated regions, but also one of the Spanish communities with the highest levels

of EP, outdated homes, and lowest employment rates. A 2021 census indicated that 8,472,407 residents live here. Moreover, recent surveys revealed that more than 20% of these habitants claimed that they currently live in

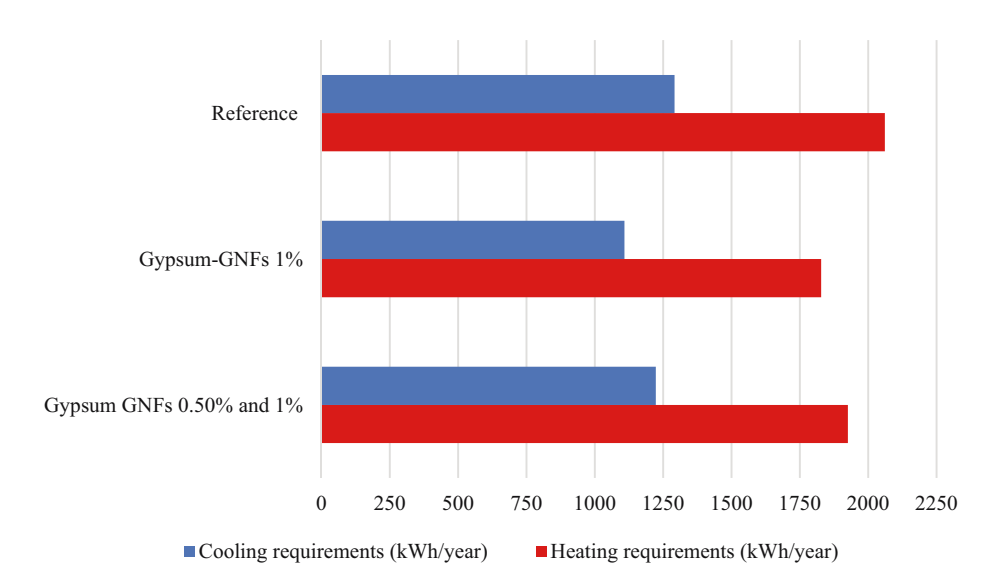


Figure 11: Annual heating and cooling demands implementing different envelope arrangements.

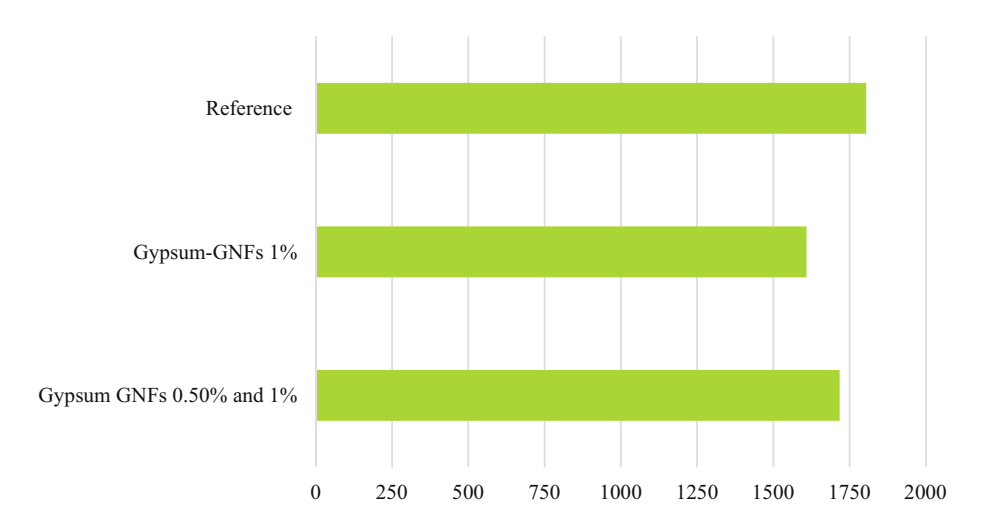


Figure 12: Annual CO₂ emissions at different envelope arrangements.

uncomfortable homes with signs of humidity and leaks. This only demonstrates the fragile situation of this region and the need to act upon this with proper answers in order to lower energy demands and improve inner room conditions. Therefore, modifying the building envelope is considered one of the most decisive actions to ensure adequate air quality and good insulation [49–52].

The values for annual heating and cooling requirements are shown in Table 10. Composites containing 1% GNFs resulted as the most efficient solution for this building when implemented in all surfaces. Reductions of 11 and 14% were obtained for heating and cooling demands, when compared to common gypsum. Furthermore, a decrease in $\rm CO_2$ emissions and total energy per building area of 11 and 9% was also reported, as illustrated in Figures 11 and 12.

4 Conclusions

This work has performed a thermomechanical characterization of a gypsum composite containing the benefits of GNFs focused on the development of building components capable of improving user comfort while lowering energy requirements, and the main conclusions are summed up as follows:

• Introducing GNFs in a gypsum mixture will change the final coloration to gray in the function of the content of the additive present in the system. Furthermore, the bulk density increases with GNF concentration up to 6%, obtaining values within the range of common gypsumbased products, usually oscillating between 700 and 1,100 kg/m³.

- Samples containing 1% of GNFs achieved the highest values for flexural and compressive strength with increments of 23 and 42%, reaching values of 2.82 and 5.77 MPa. As a result, these composites are lighter and required less amount of additive to achieve greater values for compressive strength when compared to gypsum samples containing isostatic graphite.
- Microstructural analysis revealed that the addition of GNFs resulted in the emergence of a more ordered, uniform, and denser structure with longer crystals, reduced porosity, and enhanced mechanical properties. Similar to other studies, these nanodispersed additives served as crystallization centers, introducing extra energy into the system, which led to improved crystal seeding and growth rate.
- The addition of 1% of these nanoparticles achieved a significant reduction in thermal conductivity by >40%, reaching values of 0.199 W/mK due to the effects of intensified phonon scattering. In contrast, these values for thermal conductivity remained within the range of those obtained by implementing 10% of EPS or silica granules without compromising mechanical properties.
- Implementing these components could lead to significant reductions in energy requirements for heating and cooling by 11 and 14%, respectively, along with an 11% decrease in CO_2 emissions. This indicates that improving the building envelope can be an effective approach to enhance the air quality, insulation, and comfort of households.
- GNFs could offer the potential to create new building components with improved mechanical properties, porosity, high or low thermal conductivity, electromagnetic shielding, and building monitoring. The addition of GNFs did not result in any sedimentation or dispersion problems

during the entire process. Moreover, the use of low concentrations of GNFs is not expected to severely impact costs or the recyclability of the composite. Overall, this research demonstrates the potential for the use of GNFs in gypsum composites to create new and tailored building components that can meet the current market needs and reduce the impacts of energy poverty.

Acknowledgments: The authors would like to express their gratitude to all members of the Physics and Building Materials Lab of the Technical Building School of Madrid.

Funding information: The authors state no funding involved.

Author contributions: The authors have accepted all responsibility for the entire content of this manuscript and approved its submission.

Conflict of interest: The authors state no conflict of interest.

References

- [1] Verma A, Yadav M. Application of nanomaterials in architecture An overview. Mater Today Proc. 2021;43:2921–5.
- [2] Sharifi NP, Shaikh AAN, Sakulich AR. Application of phase change materials in gypsum boards to meet building energy conservation goals. Energy Build. 2017 Mar;138:455–67.
- [3] Mastropietro P. Energy poverty in pandemic times: Fine-tuning emergency measures for better future responses to extreme events in Spain. Energy Res Soc Sci. 2022 Feb;84:102364.
- [4] Karni J, Karni E. Gypsum in construction: Origin and properties. Mater Struct. 1995 Mar;28(2):92–100.
- [5] Harrell JA. Amarna gypsite: A new source of gypsum for ancient Egypt. J Archaeol Sci Rep. 2017 Feb;11:536–45.
- [6] Herrero MJ, Escavy JI, Bustillo M. The Spanish building crisis and its effect in the gypsum quarry production (1998–2012). Resour Policy. 2013 Jun;38(2):123–9.
- [7] Jia R, Wang Q, Feng P. A comprehensive overview of fibre-reinforced gypsum-based composites (FRGCs) in the construction field. Compos Part B: Eng. 2021 Jan;205:108540.
- [8] Lushnikova N, Dvorkin L. Sustainability of gypsum products as a construction material. In: Khatib JM, editor. Sustainability of Construction Materials (2nd edition). Woodhead Publishing; 2016. p. 643–81.
- [9] Bouzit S, Merli F, Sonebi M, Buratti C, Taha M. Gypsum-plasters mixed with polystyrene balls for building insulation: Experimental characterization and energy performance. Constr Build Mater. 2021 May;283:122625.
- [10] Flores Medina N, Barbero-Barrera MM. Mechanical and physical enhancement of gypsum composites through a synergic work of

- polypropylene fiber and recycled isostatic graphite filler. Constr Build Mater. 2017 Jan;131:165–77.
- [11] Eve S, Gomina M, Gmouh A, Samdi A, Moussa R, Orange G. Microstructural and mechanical behaviour of polyamide fibrereinforced plaster composites. J Eur Ceram Soc. 2002 Dec;22(13):2269–75.
- [12] Vasconcelos G, Lourenço PB, Camões A, Martins A, Cunha S. Evaluation of the performance of recycled textile fibres in the mechanical behaviour of a gypsum and cork composite material. Cem Concr Compos. 2015 Apr;58:29–39.
- [13] Senff L, Ascensão G, Ferreira VM, Seabra MP, Labrincha JA. Development of multifunctional plaster using nano-TiO2 and distinct particle size cellulose fibers. Energy Build. 2018 Jan;158:721–35.
- [14] Ouakarrouch M, El Azhary K, Laaroussi N, Garoum M, Kifani-Sahban F. Thermal performances, and environmental analysis of a new composite building material based on gypsum plaster and chicken feathers waste. Therm Sci Eng Prog. 2020 Oct;19:100642.
- [15] Hagiri M, Honda K. Preparation and evaluation of gypsum plaster composited with copper smelter slag. Clean Eng Technol. 2021 lun:2:100084.
- [16] Barbero-Barrera M, del M, Flores-Medina N, Pérez-Villar V. Assessment of thermal performance of gypsum-based composites with revalorized graphite filler. Constr Build Mater. 2017 Jul;142:83–91.
- [17] Serna Á, Río M, del, Palomo JG, González M. Improvement of gypsum plaster strain capacity by the addition of rubber particles from recycled tyres. Constr Build Mater. 2012 Oct;35:633–41.
- [18] Gordina A, Tokarev Y, Yakovlev G, Keriene J, Sychugov S, Mohamed AES. Evaluation of the Influence of ultradisperse dust and carbon nanostructures on the structure and properties of gypsum binders. Procedia Eng. 2013;57:334–42.
- [19] Yakovlev G, Polyanskikh I, Fedorova G, Gordina A, Buryanov A. Anhydrite and gypsum compositions modified with ultrafine manmade admixtures. Procedia Eng. 2015;108:13–21.
- [20] Papadaki D, Kiriakidis G, Tsoutsos T. Applications of nanotechnology in construction industry. In: Barhoum A, Hamdy Makhlouf AS, editors. Fundamentals of Nanoparticles. Elsevier; 2018. p. 343–70.
- [21] Tokarev Y, Ginchitsky E, Sychugov S, Krutikov V, Yakovlev G, Buryanov A, et al. Modification of gypsum binders by using carbon nanotubes and mineral additives. Procedia Eng. 2017;172:1161–8.
- [22] Pervyshin GN, Yakovlev GI, Gordina AF, Keriene J, Polyanskikh IS, Fischer HB, et al. Water-resistant gypsum compositions with manmade modifiers. Procedia Eng. 2017;172:867–74.
- [23] Rafique M, Tahir MB, Rafique MS, Hamza M. History and fundamentals of nanoscience and nanotechnology. In: Tahir MB, Rafique M, Rafique MS, editors. Nanotechnology and Photocatalysis for Environmental Applications. Elsevier; 2020. p. 1–25.
- [24] Novoselov KS. Electric field effect in atomically thin carbon films. Science. 2004 Oct 22;306(5696):666–9.
- [25] Geim AK, Novoselov KS. The rise of graphene. Nat Mater. 2007 Mar;6(3):183–91.
- [26] Novoselov KS, Fal'ko VI, Colombo L, Gellert PR, Schwab MG, Kim K. A roadmap for graphene. Nature. 2012 Oct;490(7419):192–200.
- [27] Young RJ, Kinloch IA, Gong L, Novoselov KS. The mechanics of graphene nanocomposites: A review. Compos Sci Technol. 2012 lul;72(12):1459–76.
- [28] Novo S, Fonseca C, Benavente R, Blázquez-Blázquez E, Cerrada ML, Pérez E. Effect of graphene nanofibers on the morphological,

- structural, thermal, phase transitions and mechanical characteristics in metallocene iPP based nanocomposites. J Compos Sci. 2022 Jun 1;6(6):161.
- [29] AENOR. EN 13279-1, Gypsum binders and gypsum plasters Part 1: Definitions and requirements. 2008.
- [30] AENOR. EN 13279-2, Gypsum binders and gypsum plasters Part 2: Test methods. 2014.
- [31] Herrero S. Mayor P. Hernández-Olivares F. Influence of proportion and particle size gradation of rubber from end-of-life tires on mechanical, thermal and acoustic properties of plaster-rubber mortars. Mater & Des. 2013 May;47:633-42.
- [32] Navacerrada MA, Fernández P, Díaz C, Pedrero A. Thermal and acoustic properties of aluminium foams manufactured by the infiltration process. Appl Acoust. 2013 Apr;74(4):496-501.
- [33] Cao W, Yi W, Yin S, Peng J, Li J. A novel low-density thermal insulation gypsum reinforced with superplasticizers. Constr Build Mater. 2021 Apr;278:122421.
- [34] Smirnov BM, Berry RS. Growth of bubbles in liquid. Chem Cent J. 2015 Sep 21;9(1):1-8.
- [35] Biswal A, Swain SK. Smart composite materials for civil engineering applications. In: Bouhfid R, Kacem Qaiss A, Jawaid, editors. Polymer Nanocomposite-Based Smart Materials. Woodhead Publishing; 2020. p. 197-210.
- [36] Suresh Babu K, Ratnam Ch. Mechanical and thermophysical behavior of hemp fiber reinforced gypsum composites. Mater Today Proc. 2021 Jan;259:126858.
- [37] Tao J, Wang J, Zeng Q. A comparative study on the influences of CNT and GNP on the piezoresistivity of cement composites. Mater Lett. 2020 Jan;259:126858.
- [38] Wigley TML. Chemical evolution of the system calcite-gypsumwater. Can J Earth Sci. 1973 Feb 1;10(2):306-15.
- [39] Kondratieva N, Barre M, Goutenoire F, Sanytsky M, Rousseau A. Effect of additives SiC on the hydration and the crystallization processes of gypsum. Constr Build Mater. 2020 Feb;235:117479.
- [40] Ahmadi Moghadam H, Mirzaei A. Comparing the effects of a retarder and accelerator on properties of gypsum building plaster. J Build Eng. 2020 Mar;28:101075.
- [41] Virojanadara C, Syväjarvi M, Yakimova R, Johansson LI, Zakharov AA, Balasubramanian T. Homogeneous large-area gra-

- phene layer growth on6H-SiC(0001). Phys Rev B. 2008 Dec 1;78(24):245403.
- [42] Forbeaux I, Themlin J-M, Debever J-M. Heteroepitaxial graphite on6H-SiC(0001): Interface formation through conduction-band electronic structure. Phys Rev B. 1998 Dec 15;58(24):16396-406.
- [43] Capasso I, Pappalardo L, Romano RA, Iucolano F. Foamed gypsum for multipurpose applications in building. Constr Build Mater. 2021 Nov:307:124948.
- [44] Xu C, Miao M, Jiang X, Wang X. Thermal conductive composites reinforced via advanced boron nitride nanomaterials. Compos Commun. 2018 Dec;10:103-9.
- [45] Lee KH, Kim H-S, Shin WH, Kim SY, Lim J-H, Kim SW, et al. Nanoparticles in Bi0.5Sb1.5Te3: A prerequisite defect structure to scatter the mid-wavelength phonons between Rayleigh and geometry scatterings. Acta Materialia. 2020 Feb;185:271-8.
- [46] Tan WK, Hakiri N, Yokoi A, Kawamura G, Matsuda A, Muto H. Controlled microstructure and mechanical properties of Al2O3based nanocarbon composites fabricated by electrostatic assembly method. Nanoscale Res Lett. 2019 Jul 23;14(1):1-7.
- [47] Carfora A, Scandurra G, Thomas A. Forecasting the COVID-19 effects on energy poverty across EU member states. Energy Policy. 2021 Sep;161:112597.
- [48] Čekon M, Čurpek J. A transparent insulation façade enhanced with a selective absorber: A cooling energy load and validated building energy performance prediction model. Energy Build. 2019 Jan;183:266-82.
- Instituto de Estadística y Cartografía de Andalucía. Padrón municipal de habitantes [Internet]. [cited 2022 Oct 18]. https://www. juntadeandalucia.es/institutodeestadisticaycartografia/badea/ operaciones/consulta/anual/6782?CodOper=b3_128& codConsulta=6782.
- [50] Clavijo-Núñez S, Herrera-Limones R, Rey-Pérez J, Torres-García M. Energy poverty in Andalusia. An analysis through decentralised indicators. Energy Policy. 2022 Aug;167:113083.
- [51] Domínguez-Amarillo S, Fernández-Agüera J, Sendra JJ, Roaf S. The performance of Mediterranean low-income housing in scenarios involving climate change. Energy Build. 2019 Nov;202:109374.
- [52] Bienvenido-Huertas D, Sanz Fernández A, Sánchez-Guevara Sánchez C, Rubio-Bellido C. Assessment of energy poverty in Andalusian municipalities. Application of a combined indicator to detect priorities. Energy Rep. 2022 Nov;8:5100-16.